Enhancing Reliability of Inertial Measurement Unit Sensors in Quadrotor Drones

Yau-Ren Shiau[1] and Wei-Cheng Chang[1,2*]

[1]Department of Industrial Engineering and System Management, Feng Chia University,
No. 100, Wenhua Rd., Xitun Dist., Taichung City 407102, Taiwan, R.O.C.
[2]Department of Aeronautical Engineering, Chaoyang University of Technology,
No. 168, Jifeng E. Rd., Wufeng Dist., Taichung City 413310, Taiwan, R.O.C.

In unmanned aerial vehicles (UAVs), an inertial measurement unit (IMU) sensor is essential for maintaining stability and navigational accuracy during flight. It becomes exceptionally crucial when UAVs undertake complex tasks, such as flying near wind turbines for inspections or maintaining precise formations alongside other UAVs. The main challenge stems from the nonlinear nature of IMU sensor readings, especially in situations requiring meticulous control. In this article, the authors suggest integrating an unscented Kalman filter (UKF) with a support vector machine (SVM) to predict defects for effective fault prediction in UAVs. The efficacy of this method is validated through comparative experiments with standard prediction algorithms, demonstrating its accuracy in various simulated faulty scenarios. As a result of this research, the proposed method can serve as a trend predictor for monitoring IMU failures as well as a method of enhancing the reliability of drones.

1. Introduction

As technology rapidly advances, devices are evolving at an extraordinary pace. Today's machines are increasingly versatile and intelligent, yet this evolution introduces new challenges. The complexity of modern devices makes them more vulnerable to external effects, leading to the potential wear and tear of internal components and unexpected breakdowns, incurring additional costs as a result. Consequently, researchers have increasingly focused on improving the detection and diagnosis of such faults, arousing significant interest from academia and industry. Researchers from around the world are dedicated to exploring fault detection and diagnosis in depth. They aim for cost-effective and efficient solutions that minimize initial testing and trial costs through thorough research and data analysis.

In recent years, drones, also known as unmanned aerial vehicles (UAVs), have emerged as a significant area of interest and extensive research. Drones distinguish themselves from traditional aircraft, such as helicopters and airplanes, with their lightweight design and agility, making them suitable for various applications while ensuring lower operational costs.

Drones are widely adopted in various sectors, including entertainment and commerce, and significantly affect disaster management strategies. The inertial measurement unit (IMU) is crucial in enhancing the accuracy and efficiency of drone operations, particularly when UAVs experience GPS signal loss. It delivers critical data concerning the drone's velocity, direction, and the effects of gravity, which are instrumental in defining its path and stability during flight.[1]

The widespread application of drones increases the likelihood of accidents correspondingly. In response, the U.S. Federal Aviation Administration (FAA) and the European Union Aviation Safety Agency (EASA) began implementing drone-related laws and regulations in 2016. These agencies also formulated guidelines for documenting drone-related mishaps. The FAA took a step further by collaborating with the University of Abraham on an in-depth study. Reports suggest that malfunctions in navigation and positioning systems have led to drones colliding in midair. Furthermore, mechanical issues, especially concerning power, propellers, and rotor blades, have caused drones to crash into homes, resulting in significant property and agricultural damage. Moreover, there are documented cases of improper drone usage causing physical injuries to infants, brides, and even wildlife, highlighting the importance of adequate training, safety precautions, and a proper maintenance scheme.

In both traditional industrial sectors and the aerospace field, employing hardware redundancy techniques is a common strategy to minimize the risks associated with flight safety incidents that can be caused by mechanical component or sensor failures. These techniques substantially reduce the likelihood of catastrophic failure in primary systems. The common method in commercial and military aviation involves leveraging triple redundancy—or even higher levels of redundancy—in hardware components to ensure a robust safety net, significantly elevating the reliability and safety of flight operations.

While hardware redundancy offers a convenient and straightforward approach to enhancing system reliability, especially from the standpoints of implementation and management, it is not without its challenges. Hardware redundancy increases the overall system weight and battery consumption rate, which is particularly concerning for long-duration missions. Financially, redundancy measures entail the cost of extra hardware and higher long-term maintenance costs. Also, the decreasing available payload capacity can limit the aircraft's operational flexibility.[2] These challenges and trade-offs are particularly significant in the context of small UAVs (SUAVs). In smaller platforms, where weight, energy efficiency, and cost-effectiveness are highly valued, incorporating hardware redundancy necessitates a careful balancing act with these limitations.

The fault prediction method based on filtering algorithms creates a residual series through the analysis of the angular rate estimated using gyro measurement values. Subsequently, it utilizes the amplitude trends of the residual series to forecast potential faults. Typically, the filtering algorithm leverages kinetic equations to ascertain the angular rate. Furthermore, quadrotor UAV is characterized as a nonlinear system, primarily owing to its dynamic motion patterns. This configuration facilitates the integration of multiple inputs and outputs (MIMO), enhancing the system's versatility and adaptability.[3]

The aim of this study is to establish a fault early-warning mechanism to alert drone owners to the need for appropriate preventive maintenance and repairs when specific failure rates arise. The construction of the predictive model involves the steps shown in Fig. 1.

The Kalman filter (KF), developed by R. E. Kalman in 1960, is recognized as an optimal recursive data processing algorithm. It has become a benchmark in optimal estimation, leveraging the data collected over time to more precisely estimate unknown variables and their nonlinear derivatives across various systems. The KF is particularly valuable when sensors within dynamic systems might be unreliable, making state estimation methods incorporating input evaluation highly recommended. As such, the KF has gained widespread acceptance, notably in estimating angular rates and analyzing attitude kinematic equations, particularly for IMU fault prediction.[4]

We adopted an unscented KF (UKF) with the support vector machine (SVM) for IMU fault prediction because of its key characteristics that differentiate it from other filtering techniques such as the extended KF (EKF) and the basic KF. The UKF, as a nonlinear filter, excels in estimating the state of nonlinear systems based on noisy observations. Unlike the EKF, the UKF has several unique features that make it particularly advantageous for specific applications. One of the primary benefits is its deterministic sampling approach, which effectively captures both the mean and covariance of state variables. It eliminates the need for calculating Jacobians to linearize system and observation models, simplifying the UKF's implementation in complex nonlinear systems. As such, the UKF often produces more accurate state estimates, particularly when dealing with highly nonlinear systems. Compared with the first-order Taylor series expansion employed by the EKF, the UKF captures the mean and covariance of a nonlinear transformation of a random variable more precisely.[5]

2. Mathematical Model of a Rigid-Body UAV

2.1 Orientation and position of drones

In aerospace engineering and control systems, the mathematical model of a rigid-body UAV is paramount for understanding its dynamics and designing control algorithms. This model
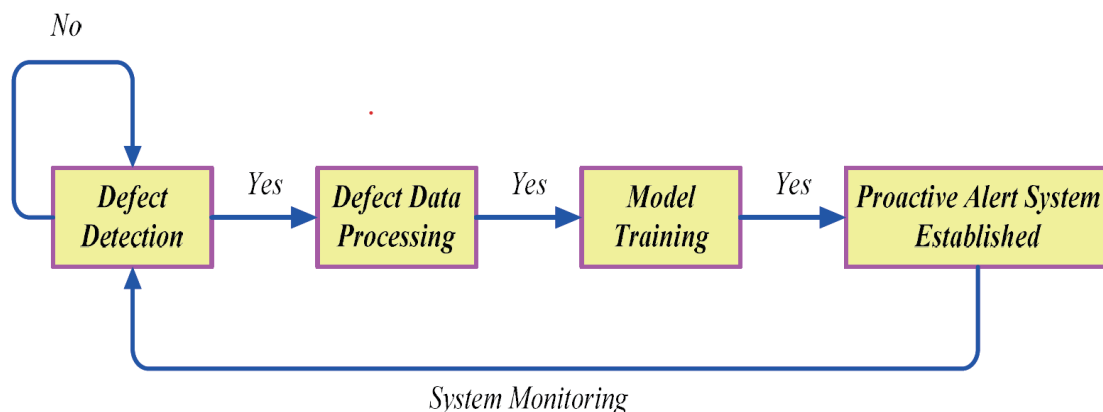
Fig. 1.   (Color online) Strategies for enhancing the reliability of IMUs.

primarily characterizes the UAV's movement in a three-dimensional space, incorporating a range of physical and aerodynamic elements. This section begins with a discussion on kinematic and dynamic equations.

Comprehending UAVs' kinematic and dynamic models is the key to developing advanced programs that accurately predict their flight behaviors This understanding also facilitates the creation of fault prediction models for these aerial systems. A standard quadrotor, for instance, exhibits six degrees of freedom (DOF): three for movements along the X-, Y-, and Z-axes, and three for rotational movements, specifically Roll (ϕ), Pitch (θ), and Yaw (ψ). The behavior of such vehicles can be explained through Newtonian physics combined with aerodynamic principles. The foundational kinematic and dynamic models that describe the movement of these rigid-body aircraft are outlined below.[6]

Various coordinate frames, such as the Earth reference frame (O_E, X_E, Y_E, Z_E) and the body fixed frame (O_B, X_B, Y_B, Z_B), play a pivotal role in pinpointing the quadrotor's position and orientation within its six degrees of freedom (6 DOF). For example, a coordinate frame affixed to the quadrotor must be utilized to assess motion equations. Nevertheless, the forces and moments exerted on the quadrotor and the values from the IMU sensors are analyzed in relation to its body frame. The position and velocity of the quadrotor are ultimately determined by an inertial frame located at the base station. As a result, three primary reference frames are established, as depicted in Fig. 2.

The equations for the motion of the UAV are calculated with reference to the aircraft's body frame. During calculations, the body's orientation and position cannot be defined within a moving frame, or else complexity will increase. Instead, a fixed frame, such as the Earth frame system, is a relatively ideal method to tackle challenge. To accomplish the transformation between two coordinate frames, the aircraft's orientation is defined by a sequence of three consecutive rotations known as Euler angles.[7,8] The equations are below.
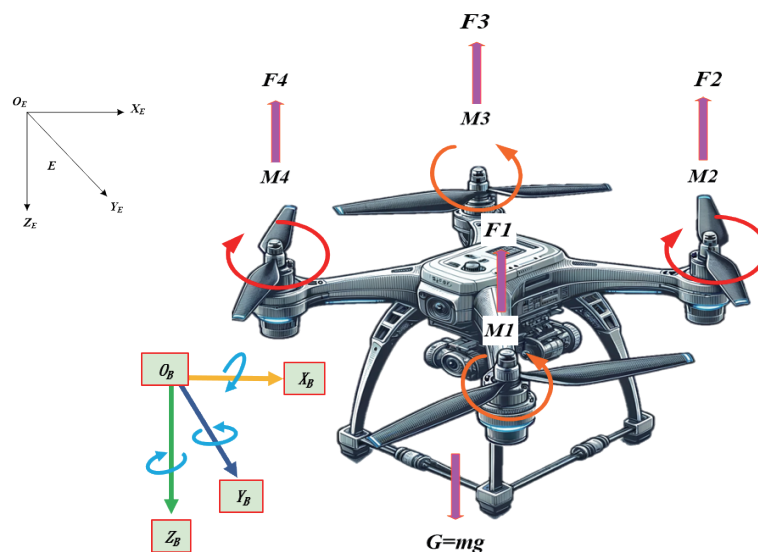
Fig. 2.   (Color online) Simplified Euler angle representation for quadrotor UAV.

$$R_x(\phi) = \begin{bmatrix} 1 & 0 & 0 \\ 0 & \cos\phi & \sin\phi \\ 0 & -\sin\phi & \cos\phi \end{bmatrix}, R_y(\theta) = \begin{bmatrix} \cos\theta & 0 & -\sin\theta \\ 0 & 1 & 0 \\ \sin\theta & 0 & \cos\theta \end{bmatrix}, R_z(\psi) = \begin{bmatrix} \cos\psi & \sin\psi & 0 \\ -\sin\psi & \cos\psi & 0 \\ 0 & 0 & 1 \end{bmatrix} \quad (1)$$

The conception in the following Eq. (2) is the product of combining these matrices.

$$R_B^E(\phi,\theta,\psi) = R_x(\phi) \cdot R_y(\theta) \cdot R_z(\psi) \quad (2)$$

The direction cosine matrix (DCM) is the rotation matrix that transforms coordinates from the body frame to the inertial frame. This matrix is a function of the Euler angle and is composed as

$$R_B^E(\phi,\theta,\psi) = \begin{bmatrix} \cos\theta\cos\psi & \cos\psi\sin\theta\sin\phi - \sin\psi\cos\phi & \cos\psi\sin\theta\cos\phi + \sin\psi\sin\phi \\ \cos\theta\sin\psi & \sin\psi\sin\theta\sin\phi + \cos\psi\cos\phi & \sin\psi\sin\theta\cos\phi - \cos\psi\sin\phi \\ -\sin\theta & \sin\phi\cos\theta & \cos\phi\cos\theta \end{bmatrix}. \quad (3)$$

The IMU delivers angular rate measurements, represented by the roll rate (p), pitch rate (q), and yaw rate (r). They are essential for determining changes in Euler angles (ϕ, θ, and ψ) that describe the body's orientation in space. The kinematic equations that link the IMU angular rates with the time derivatives of the Euler angles are given by

$$\begin{bmatrix} \dot{\phi} \\ \dot{\theta} \\ \dot{\psi} \end{bmatrix} = \begin{bmatrix} 1 & \sin\phi\tan\theta & \cos\phi\tan\theta \\ 0 & \cos\phi & -\sin\phi \\ 0 & \sin\phi\sec\theta & \cos\phi\sec\theta \end{bmatrix} = \begin{bmatrix} \ \\ \ \\ \ \end{bmatrix}. \quad (4)$$

2.2 State estimate

The nonlinear nature of UAV flight motion often necessitates using a KF for sensor fusion. Among various KFs, the UKF is particularly adept at handling systems with complex, nonlinear dynamics and measurement functions. In contrast to the EKF, which linearizes these functions, the UKF adopts the unscented transformation technique. This method enables a more accurate propagation and updating of probability distributions using Gaussian random variables (GRVs), particularly in nonlinear situations. The UKF's advanced algorithm functions as a recursive filter, efficiently dealing with nonlinear system dynamics. It avoids the complex linearization process, usually associated with the computation of Jacobian matrices, which is not only resource-intensive but also susceptible to errors, especially in intricate nonlinear systems.[9,10]

The governing equations of the UKF embody its core principles and define its functionality. During the unscented transformation (UT) phase, a crucial step is to select strategic sigma points around the mean. These points are carefully chosen to represent the mean and covariance of the Gaussian distribution accurately. This step is vital for the method's thoroughness and

efficacy in later stages. The following theoretical step is adopted to implement this recursive algorithm.

$$\hat{x}_0 = E[x_0] \tag{5}$$

$$p_0 = E\left[(x_0 - \hat{x}_0)(x_0 - \hat{x}_0)^T\right] \tag{6}$$

In this context, $\hat{x}_0$ represents the initial estimate of the state, p_0 refers to the initial covariance matrix, and $E[x_0]$ is the forecasted value of the preliminary state.

$$k \in \{1, \cdots, \infty\} \tag{7}$$

$$x_{k-1} = \left[\widehat{x}_{k-1} \ \widehat{x}_{k-1} \pm \sqrt{(L+\lambda)\hat{p}_{k-1}}\right] \tag{8}$$

The selection of sigma points is based on the estimated state covariance matrix. When calculating sigma points, $\widehat{x}_{k-1}$ represents the matrix of the evaluated state vector, while $\hat{p}_{k-1}$ is the predicted covariance matrix state at the time step $k-1$. The composite scaling parameter γ is used to calculate the square root of the scaled covariance matrix. Moreover, L represents the dimension of the augmented state vector and is involved in the computation of sigma points. Note that the scaling parameter λ specified in Eq. (8) is different from γ and determines the spread of the sigma points.

The UKF uses a recursive algorithm to optimally filter the state. It considers various factors from the previous state, such as noise, the time elapsed between measurements, and input and output data. These elements are updated regularly. The procedure for information prediction and correction is as follows.

(a) Time update process—State Prediction

$$X^x_{k|k-1} = f\left(X^x_{k|k-1}, u_{k-1}, (X^v_{|k-1})\right) \tag{9}$$

$$\hat{x}^-_k = \sum_{i=0}^{2L} w_i^{(m)} X^x_{i,k|k-1} \tag{10}$$

$$P^-_k = \sum_{i=0}^{2L} w_i^{(c)} \left(X^x_{i,k|k-1} - \hat{x}^-_k\right)\left(X^x_{i,k|k-1} - \hat{x}^-_k\right)^T \tag{11}$$

$$Y_{k|k-1} = H\left(X^x_{k|k-1}, X^n_{k|k-1}\right) \tag{12}$$

$$\hat{y}^-_k = \sum_{i=0}^{2L} w_i^{(m)} Y^x_{i,k|k-1} \tag{13}$$

(b) Measurement update process—State Correction

$$P_{\hat{y}_k\,y_k} = \sum_{i=0}^{2L} w_i^{(c)} \left(Y_{i,k|k-1} - \hat{y}_k^- \right)\left(Y_{i,k|k-1} - \hat{y}_k^- \right)^T \tag{14}$$

$$P_{x_k\,y_k} = \sum_{i=0}^{2L} w_i^{(c)} \left(X_{i,k|k-1} - \hat{x}_k^- \right)\left(Y_{i,k|k-1} - \hat{y}_k^- \right)^T \tag{15}$$

$$K_k = P_{x_k y_k} \left(P_{\tilde{x}_k \tilde{y}_k} + R \right)^{-1} \tag{16}$$

$$P_k = P_k^- - K_k \left(P_{\tilde{x}_k \tilde{y}_k} + R \right) K_k^T \tag{17}$$

$$\hat{x}_k = \hat{x}_k^- + K_k \left(y_k - \hat{y}_k^- \right) \tag{18}$$

In summary, the equations listed in procedures (a) and (b) iteratively predict the state of a system at a future time and then update those predictions with new measurements. The Kalman gain in Eq. (16) is a key component that balances the weight given to new measurements versus the predictions. Equation (17) is concerned with updating the state covariance to reflect the new confidence level after incorporating the measurement. Finally, the state estimate is updated using the Kalman gain and measurement residual, as shown in Eq. (18).

2.3 Flight reconstruction

In the coming phase, UKF will be used to reconstruct the actual flight path, and two critical parameters, the process noise covariance matrix (Q) and the measurement noise covariance matrix (R), will be used to adjust the completed flight log. The root mean square error (*RMSE*) will be adopted to compare the predictive performance characteristics of UKF and EKF for subsequent fault prediction purposes.

RMSE is employed to assess the quality of the adjusted data to confirm its suitability for model training. The equation representing *RMSE* is

$$RMSE = \sqrt{\frac{1}{n} \sum_{i=1}^{n} (y_1 - y_2)^2}. \tag{19}$$

The 2D and 3D flight patterns respectively depicted in Figs. 3 and 4 illustrate the reconstructed flight paths using IMU sensor data. Simulations were carried out to showcase the capabilities of the UKF and EKF in making accurate estimates despite limited measurement data. The estimation results show discrepancies compared with the actual measurement data, presenting the findings as estimated coordinates and linear velocities.
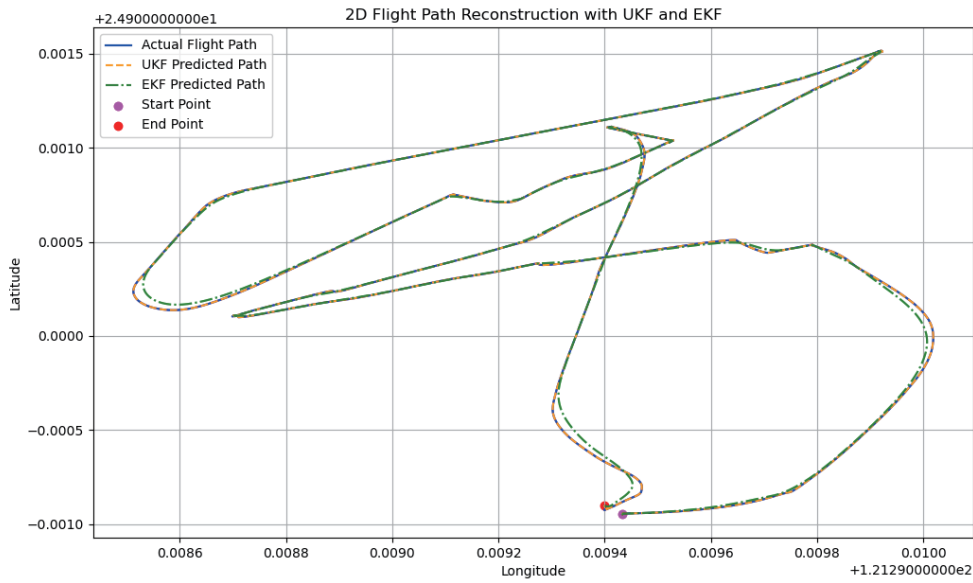
Fig. 3.   (Color online) Flight path reconstruction in 2D pattern.
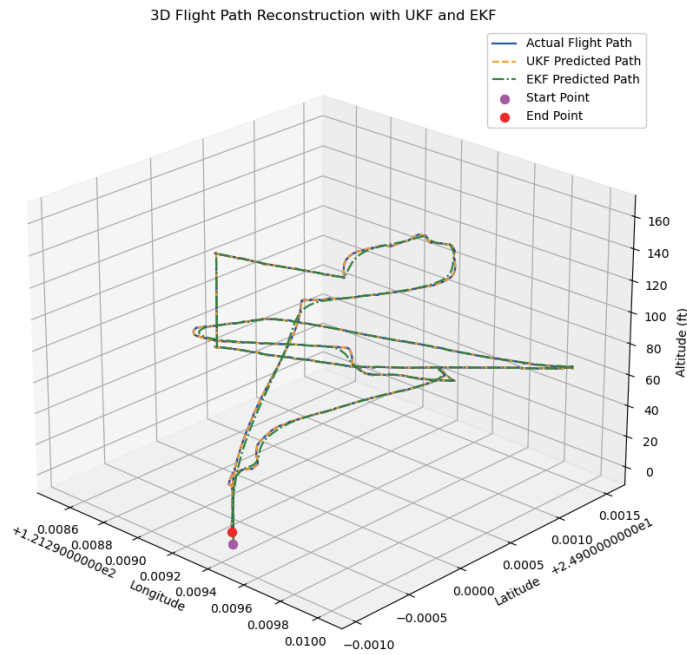
Fig. 4.   (Color online) Flight path reconstruction in 3D pattern.

Table 1 shows the original flight data and the predicted flight paths obtained using the UKF and EKF. The UKF, after extra tuning the parameters using the sigma point calculation method proposed by Wan and van der Merwe,[11] demonstrated a significantly lower *RMSE* than the EKF. Therefore, the UKF will be used in future research for fault prediction since it performs better than the EKF.

Table 1
RMSE values obtained using UKF and EKF.

	UKF	EKF
Latitude (deg)	1.775886	3.481463
Longitude (deg)	1.296059	2.499633
Altitude (ft)	0.163879	3.028826

3.   Prognostic and Health Management

3.1   Defect injection

In practical applications, various IMUs exhibit distinct tolerances to a range of stochastic processes. Academic studies have identified common categories of IMU faults. These categories, sequentially arranged, include (i) Normal Condition, indicating a healthy situation; (ii) Sensor Bias, referring to consistent measurement deviation; (iii) Drifting, where readings change erratically over time; (iv) Inaccuracy, denoting a decrease in measurement precision; (v) Sensor Freezing, where the sensor fails to record changes; and (vi) Calibration Error, related to incorrect sensor calibration.[12,13] These fault symptoms can be expressed as

$$S_i(t) = \begin{cases} T_i(t), \text{ for all } t > 0 \\ T_i(t) + d_i, d_i(t) = 0, d_i(tF_j) \neq 0 \\ T_i(t) + d_i(t), |d_i(t)| \leq \lambda_i t, 0 < \lambda_i \ll 1, \text{for all } t \geq tF_j \\ T_i(t) + d_i(t), |d_i(t)| \leq d_i, d_i(t) \rightarrow 0, \text{ for all } t \geq tF_j \\ T_i(tF_i), \text{ for all } t \geq tF_i \\ C_i T_i(t). \text{ for all } t \geq tF_i. \end{cases} \quad (20)$$

These equations demonstrate common failure patterns of IMU sensors in a mathematical way, comparing the sensor reading $S_i(t)$ with the true value $T_i(t)$. The term tF_i represents the time instant when the failure occurrs in sensor i, and d_i is the accuracy coefficient. C_i reveals the effectiveness coefficient and λ_i represents the drift rate.

The upcoming research uses the dataset obtained from the faults randomly injected into the original dataset, as mentioned above, to train a health prediction model, where the UKF with the SVM is adopted in experiments. Figure 5 shows various fault patterns indicated in Eq. (20) using visualization techniques.

3.2   Data processing

The dataset is cleaned by the following commonly employed methods,[14] and the visualized results are shown in Fig. 6:
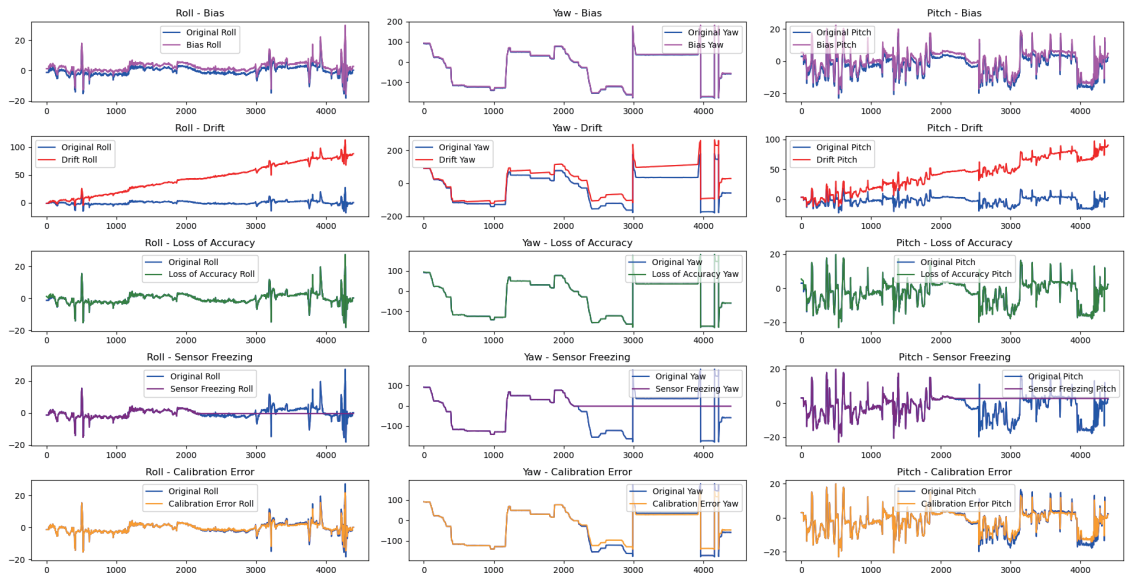
Fig. 5.   (Color online) Defect simulation for model training.
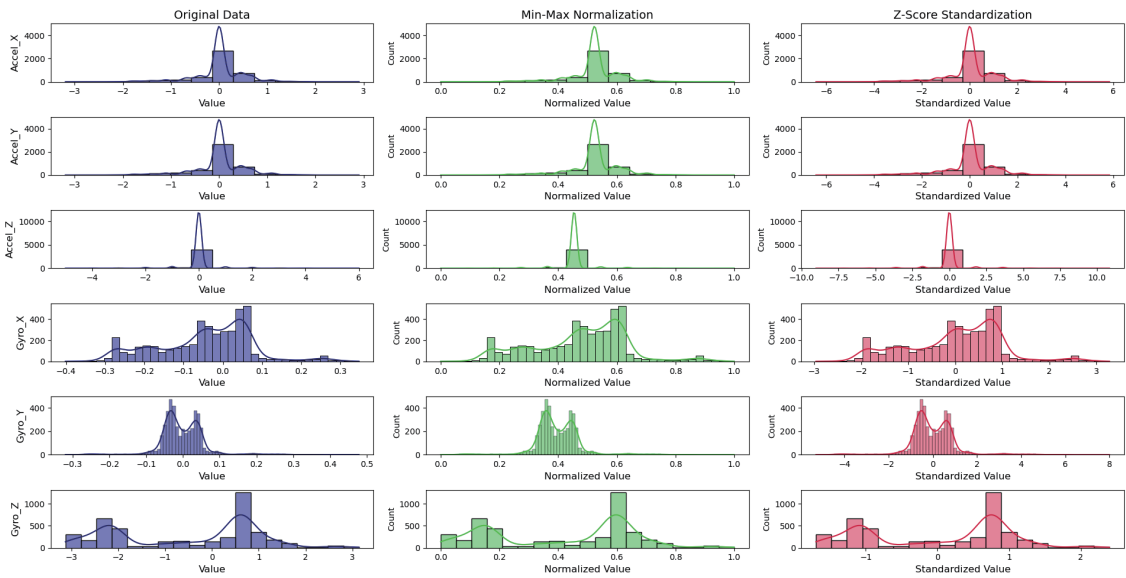
Fig. 6.   (Color online) Histograms for data standardization and normalization.

(a) Data normalization:

$$X_{normal} = \frac{x - x_{min}}{x_{max} - x_{min}} \in [0,1].$$

$$(21)$$

(b) Data standardization:

$$Z_{score} = \frac{x - \mu}{\sigma} \sim N.$$

(22)

In these equations, x denotes the original data, μ represents the mean of the data, and σ signifies the standard deviation. The described procedure rescales the data to fall within the interval of (0, 1), ensuring it follows a standard normal distribution.

3.3 Model training and validation

The following steps show a combination of the characteristics of the UKF with SVM techniques to improve the accuracy of various IMU fault predictions. The objective is to provide a relatively reliable and high-performance fault classification model by capitalizing on UKF characteristics in dealing with nonlinear systems and the SVM's solid foundation for classification tasks. This approach is expected to enhance the overall system stability and improve the performance robustness in dynamic environments. Furthermore, after several experiments, it was discovered that SVM produces better predictive results in this experiment when using the radial basis function (RBF) as the kernel. Equation (23) is the fundamental theory of the RBF.[15–17]

$$k(x_i, x_j) = \exp\left(-\frac{\left\|x_i - x_j\right\|^2}{2\sigma^2}\right)$$

(23)

Here, $k(x_i, x_j)$ is the RBF kernel function, $\left\|x_i - x_j\right\|$ represents the Euclidean distance between the data points x_i and x_j, and σ is the width of the Gaussian kernel.

The principal component analysis (PCA) method, proposed by Karl Pearson in 1901, is employed for dimensionality reduction in the following steps before model training. PCA is a statistical approach that uses linear algebra to derive solutions without predefined parameters. It involves straightforward calculations of statistical measures, such as the mean and covariance, directly from the data without any prior assumptions.[18] Figure 7 and Table 2 show the experimental and fault classification results.

Three key metrics adopted to evaluate the SVM classifier were precision, recall, and F1-score. Precision measures the accuracy of the model's positive predictions, indicating the proportion of true positive results among all positive classifications. Recall or sensitivity assesses the model's ability to identify all positive cases, reflecting the true positive rate. The F1-score, a harmonic mean of precision and recall, is a balance between the two and is suited to scenarios with uneven class distributions. These metrics collectively provide a comprehensive assessment of the model's performance in binary classification tasks.[19]
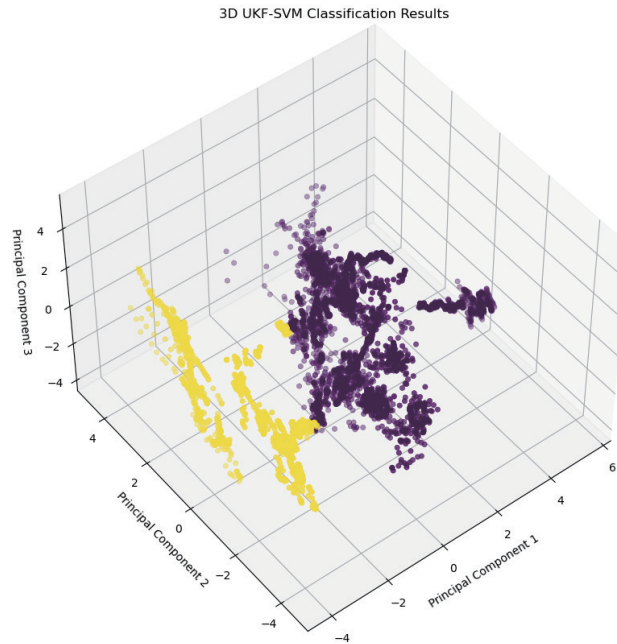
Fig. 7. (Color online) 3D UKF-SVM classification results.

Table 2
UKF-SVM classification accuracy report for different kernels.

Classification Accuracy Report			
	Precision	Recall	F1-score	Sample
0	0.99	0.97	0.98	1316
1	0.97	0.98	0.97	1322
Accuracy	—	—	0.98	2638
Macro avg	0.98	0.98	0.98	2638
Weighted avg	0.98	0.98	0.98	2638
Accuracy of Linear SVM on test set: 0.7845366685616828			
Accuracy of RBF SVM on test set: 0.9775952245594087			
Accuracy of Linear SVC on test set: 0.923820352472996			

3.2 Model comparison

We use the UKF-SVM method to randomly generate singular faults of various types. The comparative outcomes for each algorithm are as follows. UKF-SVM achieves a remarkable accuracy of 1.00, equal to XGBoost's accuracy of 1.00. The K-nearest neighbors (KNN) demonstrates an accuracy of 0.997382, while logistic regression records an accuracy of 0.982379. The accuracy of the random forest algorithm is 0.996683. Among these established algorithms, the UKF-SVM proposed in this study exhibits a slightly superior performance.

This approach and other common PHM algorithms are compared, and the results are visualized as below.
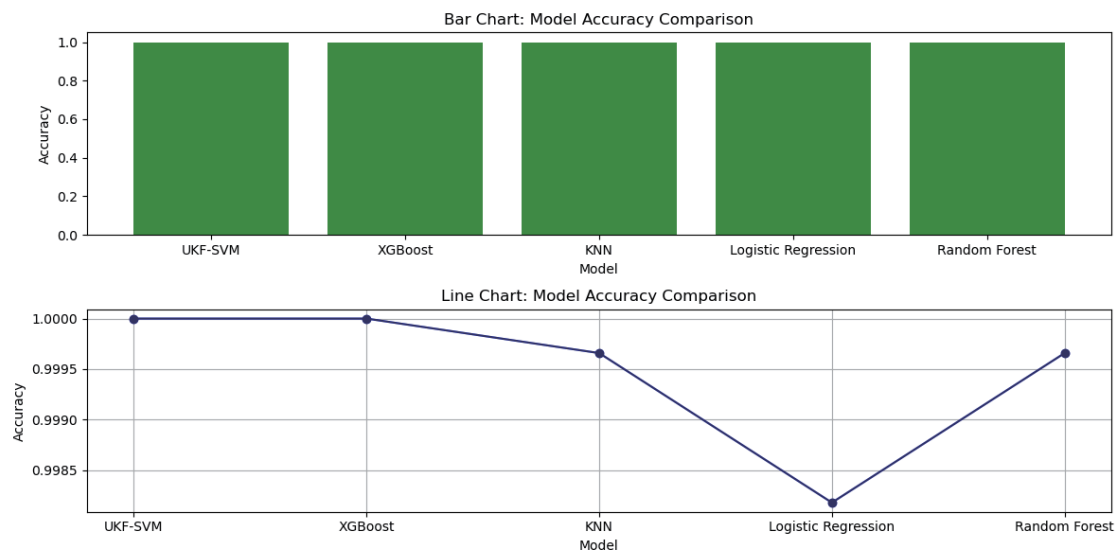
Fig. 8.   (Color online) Evaluation of accuracies of various algorithms.

4.   Conclusions

To ensure the safe operation of drones in human environments, evaluation methods such as global navigation satellite system (GNSS) and automatic dependent surveillance-broadcast (ADS-B) tracking, which are more dependable and capable of real-time processing, are required. Additionally, the high operational cost is confirmed. In this study, we conducted fault prediction analysis by the UKF-SVM method. In the real world, the operating environment of drones is continuously changing. Therefore, the approaches to data preprocessing, feature engineering, or data imputation must be adjusted in accordance with the actual situation. The fault prediction data presented in this study utilized eight flight logs, accounting for 16863 records, including normal data from accelerometer and gyroscope sensors and a database randomly inserted with various faults for training. The results of the training demonstrated satisfactory performance. Moreover, the characteristics of the UKF contribute further to predicting subsequent flight paths, thus enhancing the safety and reliability of drones.

Despite the high precision observed in the test results for prediction, the research still has certain limitations. To overcome these limitations, deploying edge devices on UAVs and transmitting real-time data through a popular lightweight messaging protocol via Internet of Things (IoT), called message queuing telemetry transport (MQTT), is recommended. These enhancements are aimed at facilitating the execution of tiny machine learning-based flight control systems to collect essential data for estimating the degradation trajectory and to assist drone owners in prioritizing maintenance decisions when long-term or critical failures occur repeatedly.[20,21]

References

1   L. R. Newcome: Unmanned Aviation: A Brief History of Unmanned Aerial Vehicles (American Institute of Aeronautics and Astronautics, 2004). https://doi.org/10.2514/4.868894

2   Y. Zhong, W. Zhang, Y. Zhang, J. Zuo, and H. Zhan: J. Intell. Rob. Syst. **96** (2019) 555. https://doi.org/10.1007/s10846-019-01002-4

3   Y. Hu, X. Miao, Y. Si, E. Pan, and E. Zio: Reliab. Eng. Syst. Saf. **217** (2022) 108063. https://doi.org/10.1016/j.ress.2021.108063

4   R. E. Kalman: J. Basic Eng. **82** (1960) 35. https://doi.org/10.1115/1.3662552

5   M. Rhudy, Y. Gu, J. Gross, and M. R. Napolitano: Int. J. Navig. Obs. **2011** (2011) 1. https://doi.org/10.1155/2011/416828

6   A. K. Sivarathri, A. Shukla, and A. Gupta: Array **17** (2023) 100269. https://doi.org/10.1016/j.array.2022.100269

7   C. Hajiyev, H. E. Soken, and S. Y. Vural: State Estimation and Control for Low-Cost Unmanned Aerial Vehicles (Springer International Publishing, Switzerland, 2015) 1st ed., pp. 9–23. https://doi.org/10.1007/978-3-319-16417-5

8   S. Du, W. Sun, and Y. Gao: Sensors **16** (2016) 12. https://doi.org/10.3390/s16122017

9   S. J. Julier and J. K. Uhlmann: Proc. SPIE Int. **3068** (1997) 182. https://doi.org/10.1117/12.280797

10   W. C. Chang and Y. R. Shiau: J. Aeronaut. Astronaut. Aviation **55** (2023) 257. https://doi.org/10.6125/JoAAA.202306_55(2S).06

11   E. A. Wan and R. Van Der Merwe: Proc. IEEE 2000 Adaptive Systems for Signal Processing, Communications, and Control Symp. (IEEE, 2000) 153–158. https://doi.org/10.1109/ASSPCC.2000.882463

12   J. D. Bošković and R. K. Mehra: Fault Diagnosis and Fault Tolerance for Mechatronic Systems: Recent Advances Vol. 1 (Springer, Berlin Heidelberg, 2003) 1st ed., pp. 129–167. https://doi.org/10.1007/3-540-45737-2_5

13   R. Puchalski and W. Giernacki: Drones **6** (2022) 330. https://doi.org/10.3390/drones6110330

14   D. Singh and B. Singh: Appl. Soft Comput. **97** (2020) 105524. https://doi.org/10.1016/j.asoc.2019.105524

15   Z.-H. Zhou: Machine Learning (Springer, Singapore, 2021) 1st ed., pp. 129–153. https://doi.org/10.1007/978-981-15-1967-3

16   E. Dilmen: IFAC-PapersOnLine **53** (2020) 8820. https://doi.org/10.1016/j.ifacol.2020.12.1392

17   S. Huang, N. Cai, P. Pacheco, S. Narrandes, Y. Wang, and W. Xu: Cancer Genomics Proteomics **15** (2018) 41. https://doi.org/10.21873/cgp.20063

18   M. Zee: A Tutorial on Principal Component Analysis (Published Online 2014). https://doi.org/10.13140/2.1.1593.1684

19   J. Arunnehru and M. Kalaiselvi Geetha: Proc. Mining Intelligence and Knowledge Exploration: First Int. Conf. (2013) 70–81. https://doi.org/10.1007/978-3-319-03844-5_8

20   E. M. Lau, G. C. Peng, W. C. Chang, and J. M. Lin: 2023 Int. Conf. Advanced Robotics and Intelligent Systems (ARIS) (IEEE 2023) 1–5. https://doi.org/10.1109/ARIS59192.2023.10268551

21   H. J. Park, N. H. Kim, and J. H. Choi: Reliab. Eng. Syst. Saf. **244** (2024) 109954. https://doi.org/10.1016/j.ress.2024.109954